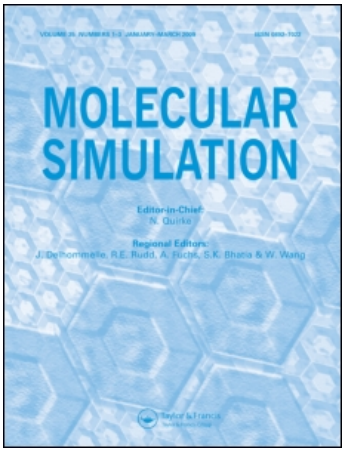

Molecular Simulation
Publication details, including instructions for authors and subscription information:
http://www.informaworld.com/smpp/title~content=t713644482

A density functional theory study on the interaction of hydrogen molecule with MOF-177

Ganga P. Dangi[a]; Renjith S. Pillai[b]; Rajesh S. Somani[a]; Hari C. Bajaj[a]; Raksh V. Jasra[b]
[a] Discipline of Inorganic Materials and Catalysis, Central Salt and Marine Chemicals Research Institute, Council of Scientific and Industrial Research (CSIR), Bhavnagar, Gujarat, India [b] Reliance Technology Group, Reliance Industries Limited, Vadodara Manufacturing Division, Vadodara, Gujarat, India

Online publication date: 16 April 2010

To cite this Article Dangi, Ganga P. , Pillai, Renjith S. , Somani, Rajesh S. , Bajaj, Hari C. and Jasra, Raksh V.(2010) 'A density functional theory study on the interaction of hydrogen molecule with MOF-177', Molecular Simulation, 36: 5, 373 — 381
To link to this Article: DOI: 10.1080/08927020903487404
URL: http://dx.doi.org/10.1080/08927020903487404

Molecular Simulation
Vol. 36, No. 5, April 2010, 373–381

Taylor & Francis
Taylor & Francis Group

A density functional theory study on the interaction of hydrogen molecule with MOF-177

Ganga P. Dangi[a], Renjith S. Pillai[b], Rajesh S. Somani[a], Hari C. Bajaj[a]* and Raksh V. Jasra[b]

[a]*Discipline of Inorganic Materials and Catalysis, Central Salt and Marine Chemicals Research Institute, Council of Scientific and Industrial Research (CSIR), G.B. Marg, Bhavnagar 364 002, Gujarat, India;* [b]*Reliance Technology Group, Reliance Industries Limited, Vadodara Manufacturing Division, Vadodara 391 346, Gujarat, India*

(*Received 20 July 2009; final version received 15 November 2009*)

The binding energies of H_2 molecule with metal-organic framework MOF-177 clusters at various possible interaction sites have been calculated using density functional theory. The binding energy of adsorbed H_2 molecule in MOF-177 was investigated, with the consideration of the favourable adsorption sites and the orientations at the inorganic cluster Zn_4O and organic linker (1,3,5-benzenetribenzoate) in order to evaluate the role of these two principal components in MOF for H_2 adsorption. Our results showed that both the inorganic connector and the organic linker play an important role in the H_2 adsorption. The binding energy calculated for the inorganic cluster is 2.96–4.50 kJ mol^{-1} and for the organic linker is 2.6–3.8 kJ mol^{-1}.

Keywords: metal-organic frameworks; MOF-177; DFT; hydrogen; binding energy

1. Introduction

Hydrogen has received much attention as a pollution-free energy source and an alternative for fossil fuels in the future. Due to the difficulty in appropriate hydrogen storage devices, it is a demanding disadvantage to use it as an automobile fuel. A wide variety of storage methods have been considered such as high-pressure containers, liquid hydrogen, metal hydrides and physisorption in porous materials [1–4]. The highly porous and greater H_2 affinity materials would be economical and safe for H_2 storage. Recently, a great deal of effort has been devoted to safe and applicable hydrogen storage materials, which should meet the requirements of high gravimetric/volumetric storage density, fast kinetics, favourable thermodynamics and reversibility.

Several materials such as zeolites, carbon-based materials such as activated carbons, carbon nanotubes, graphene and metal-organic frameworks (MOFs) have been investigated for H_2 storage. Among these, MOFs have been identified as potential candidates for hydrogen storage materials. MOFs are crystalline compounds formed through the self-assembly of metal ions or metal clusters and various bridging organic ligands. MOFs have received considerable attention as a new class of promising gas storage materials after the first report of hydrogen uptake by Yaghi and co-workers [5]. Since then, various MOFs have been synthesised and characterised for hydrogen storage applications [6]. Among various MOFs, MOF-177 synthesised by Chae et al. [7], having a Langmuir surface area of 4500 m^2 g^{-1} and a pore volume of 1.59 cm^3 g^{-1}, is the highest in the Zn-based MOFs. MOF-177 consists of a six-connected [Zn_4O] node with a three-connected tri-branched 1,3,5-benzenetribenzoate (BTB) linker. However, the crystallographic symmetry is lower for the Zn_4O $(O_2C-)_6$ cluster. Wong-Foy et al. [8] reported a Langmuir surface area of 5640 m^2 g^{-1} and gravimetric H_2 adsorption capacity of 7.5 wt% with a volumetric capacity of 32 g l^{-1} at 77 K and 70 bars, the highest capacity obtained so far in MOF-type materials for H_2 storage at 77 K.

XRD, neutron scattering and infrared spectroscopy studies have been reported in literatures in order to determine the strength of the interactions of hydrogen with the primary and secondary building units of the nanostructure [9–13]. Although binding at the metal corner is stronger, these sites get saturated very quickly, and at higher temperatures and pressures, there is a broad range of binding sites around the organic linker and the metal corners. Several grand canonical Monte Carlo (GCMC) simulation [14–19] studies have been performed in MOFs to understand the possible interaction sites, heats of adsorption and adsorption isotherm. Quantum chemical calculations have also been performed in order to elucidate the interaction of H_2 with the MOFs using various levels of functionals [20–25].

In the present work, we calculate the binding energy of hydrogen molecule with MOF-177, both at the organic linker (BTB) and inorganic cluster. Herein, we have tried to find out the effect of the organic linker on the binding energy of H_2 with the inorganic cluster. We also investigated the multiple H_2 binding at the organic linker

*Corresponding author. Email: hcbajaj@csmcri.org

ISSN 0892-7022 print/ISSN 1029-0435 online

DOI: 10.1080/08927020903487404
http://www.informaworld.com

to understand the interaction between adsorbed H_2 and the effect on the binding of further H_2 molecules.

2. Models and computational method

All cluster calculations were performed with density functional theory (DFT), within the generalised gradient approximation (GGA) using DMol3 code implemented in the 'Materials Studio' package of Accelrys, Inc. [26]. The Perdew and Wang (PW91) exchange–correlation functional [27] and all electron calculations employed with the double numerical plus polarisation (DNP) basis set [28–30] were used throughout the calculations, which is equivalent in accuracy to the commonly used 6-31G** Gaussian orbital basis set. However, the numerical basis set is much more accurate than a Gaussian basis set with the same size. The PW91 functional has been shown to perform well in describing weakly bound systems in a number of DFT studies [31–35]. The convergence criteria were set as follows: energy $= 1 \times 10^{-5}$ Ha; force $= 2 \times 10^{-3}$ Ha/Å; displacement $= 0.005$ Å.

The unit cell structure of MOF-177 (Figure 1) was constructed from the refined single-crystal data reported by Chae et al. [7]. The unit cell contains eight $Zn_4O(BTB)_2$, which is too large for the calculation. Therefore, to reduce the computational time, a simplified cluster model from the unit cell of MOF-177 was constructed. For the calculation of H_2 binding energy at the organic linker model, as shown in Figure 2(a), the MOF-177 cluster model was constructed and the termination was saturated with the methyl groups, while for the calculation of H_2 binding energy at the inorganic cluster model, as shown in Figure 2(b), the MOF-177 cluster model was constructed where six BTB organic linker groups were attached to the inorganic cluster. Our approach to construct the model is similar to the previously reported work [14,22], and presents a seamless representation including metal centre and organic linker for tracing all the possible adsorption positions. All the calculations, geometry optimisation and energy calculations were performed using the DFT/PW91 method. The coordinates of the host system were not held fixed during the geometry optimisations of all models. The orientation of the H_2 molecule with the model structures was also unconstrained.

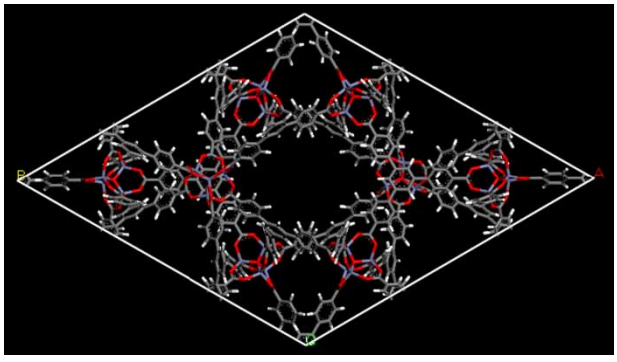

Figure 1. Unit cell structure of MOF-177.

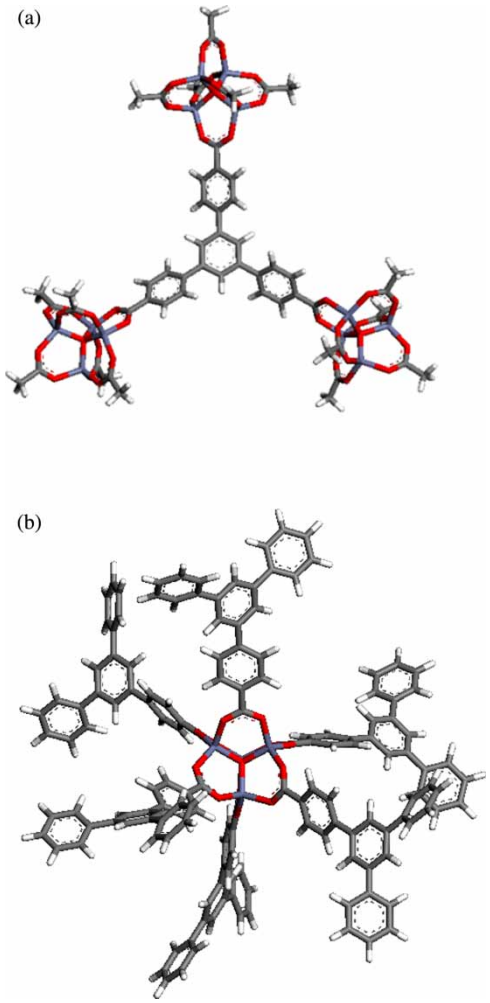

Figure 2. (a) MOF-177 cluster model used for the calculations of H_2 binding at the organic linker. (b) MOF-177 cluster model used for the calculations of H_2 binding at the inorganic cluster.

3. Results and discussion

The total binding energies (BE) of the H_2 molecules are calculated from Equation (1), and the consecutive binding energy (CBE) of the nth H_2 molecule vs. the other $(n-1)$ H_2 molecules from Equation (2),

$$\mathrm{BE} = E_{\mathrm{Host}-(\mathrm{H_2})_n} - E_{\mathrm{Host}} - nE_{\mathrm{H_2}}, \quad (1)$$

$$\mathrm{CBE} = \mathrm{BE}_n - \mathrm{BE}_{n-1}, \quad (2)$$

where E_{Host} and $E_{\mathrm{H_2}}$ are the total electronic energies of the MOF cluster model and the hydrogen molecule, respectively; $E_{\mathrm{Host}-(\mathrm{H_2})_n}$ is the total electronic energy of the $n\,H_2$

molecules adsorbed over the MOF cluster model and n is the number of the adsorbed H_2 molecules. Interactions of the H_2 molecule with the organic linker and the inorganic cluster have been studied with perpendicular and parallel orientations of the H_2 molecule. For the H_2 interaction with the organic linker, we have used the model shown in Figure 2(a) and for the H_2 interaction with the inorganic cluster, we have used the model shown in Figure 2(b), but for the sake of clarity only the organic linker (Figure 3) and the inorganic cluster (Figure 5) are shown.

3.1 H_2 binding energy with the organic linker

The H_2 binding energy with the organic linker at several sites such as above the C_6H_3 phenylene face (central ring), above the C_6H_4 phenylene face (side rings), on the CH_2 phenylene edge and towards the hydrogen atom of the central ring was calculated. The parallel and perpendicular orientation of the H_2 molecule at each site was studied. The optimised structures with adsorbed H_2 molecule on the organic linker are shown in Figure 3 and the binding energies of H_2 with the organic linker are given in Table 1.

H_2 above the C_6H_3 phenylene face (central ring) in perpendicular orientation to the plane of the ring is named as model I (Figure 3). H_2 above the C_6H_3 phenylene face (central ring) in parallel orientation to the plane of the ring is named as model II. The binding energy of H_2 above the C_6H_4 phenylene face in perpendicular orientation to the plane of the ring (model I) is stronger than the H_2 in parallel orientation (model II). Also, the binding energy of H_2 above the C_6H_4 phenylene face (side ring) in perpendicular orientation to the plane of the ring (model III) is stronger than the H_2 in parallel orientation (model IV). This showed that the interaction of H_2 at the centre of the rings is stronger for the perpendicular orientation rather than the parallel interaction. The interaction of H_2 at the central ring was stronger than the side ring. This may be due to the difference in the electronic environment of the two rings.

The interaction of H_2 in the plane and perpendicular to the plane of the ring at the CH_2 phenylene edge (model V) is stronger than the parallel orientation of H_2 (model VI). For models VII–X, front views and side views are shown in Figure 3 for clear visualisation. The highest binding energy of 3.80 kJ mol^{-1} was observed at the edge of the three rings (model VII) and H_2 is at the edge of the C_6H_3 phenylene ring (central ring) and in the plane of the ring (model IX). At these sites, H_2 interacts with three hydrogen atoms of the rings which led to the strong binding energy. The H_2 binding energy can be increased by the functionalisation of the organic linker.

The potential energy curves of H_2 to the organic linker (BTB) for different models are shown in Figure 4. The x-axis represents the distance between the centre of H_2 and the centre of the rings for models I–IV and the distance between the centre of H_2 and the closest hydrogen atom of the central ring for models VII–X.

3.2 H_2 binding energy with the inorganic cluster

At the inorganic cluster, there are three main adsorption sites: α, β and γ as proposed by Rowsell et al. [11] from the inelastic neutron-scattering study and also by Klontzas et al. [23] and Kuc et al. [25] from theoretical calculations. Here, we have also calculated the binding energy at three sites, i.e. α, β and γ. The optimised structures with the adsorbed H_2 molecule on the inorganic cluster are shown in Figure 5 and the binding energies of H_2 with the inorganic cluster are given in Table 2.

The strongest binding energy of 4.50 kJ mol^{-1} was obtained at the α-site, where the H_2 molecule is above one face of the octahedral inorganic cluster, equidistant to three carboxylates and oriented perpendicularly to the central O—Zn bond (Figure 5(a)). The H_2 molecule interacts with three surrounding Zn ions and carboxyl group, consequently, resulting in the strongest binding energy at this site. Lee et al. [22] reported the binding energy of 4.27 kJ mol^{-1} for IRMOF-1 using the same method. Even smaller binding energy of 3.1 kJ mol^{-1} was found for this site by Klontzas et al. [23] at the IR-MP2/TZVPP level using the model in which the benzenedicarboxylate (BDC) linker was substituted by hydrogen. The interaction of H_2 in perpendicular orientation at the α-site is stronger than the parallel orientation because, at the parallel orientation, only one H-atom has many close contacts to the host structure. The binding energy observed at the β-site is weaker than that observed at the α-site. At the β-site, H_2 is above the face of a ZnO_4 tetrahedron, oriented perpendicularly to the central Zn—O bond (Figure 5(c)). For IRMOF-1 at this site, Lee et al. [22] reported the binding energy of 3.05 kJ mol^{-1}, and that of 1.34 kJ mol^{-1} was reported by Klontzas et al. These results clearly demonstrate that the binding energy of H_2 at the inorganic cluster is influenced by the organic linker. At the β-site, the parallel interaction of H_2 is stronger than the perpendicular one. The binding energy observed at the γ-site is weaker than the α- and β-sites. In the γ-site, the H_2 molecule is above the edge of a ZnO_4 tetrahedron. The interaction of H_2 in the perpendicular orientation (Figure 5(e); with respect to the centre of the O—O edge of the ZnO_2 triangle), at the γ-site, is stronger than that in the parallel one because the parallel orientation of H_2 at the γ-site is not stable and it becomes slightly perpendicular after geometry optimisation (Figure 5(f)). The α- and β-binding sites are the most preferable to be occupied followed by the γ-site. At the α- and γ-sites, the perpendicular orientation of H_2 is more favourable, while at the β-site, the parallel orientation of H_2 is more favourable. Our results showed that the H_2 binding energy at the inorganic cluster is effected by the organic linker.

(I)

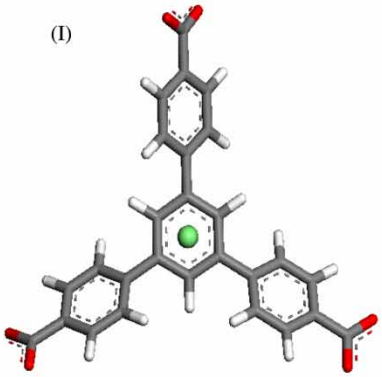

(II)

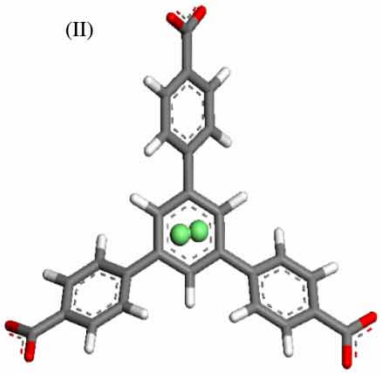

(III)

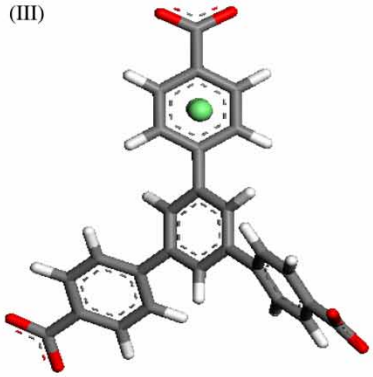

(IV)

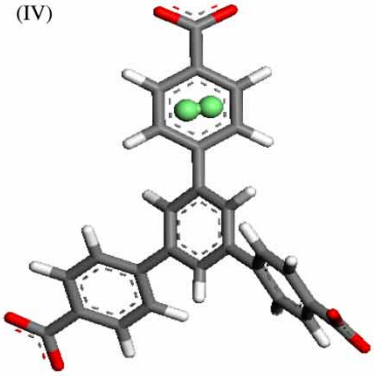

(V)

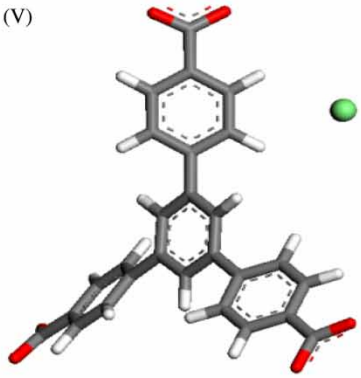

(VI)

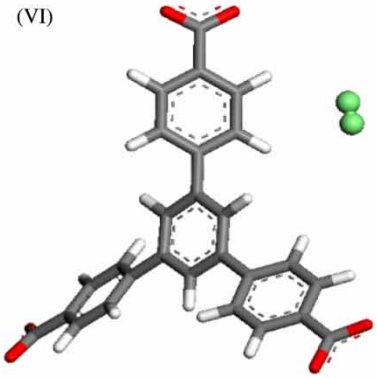

(VII a)
Front view

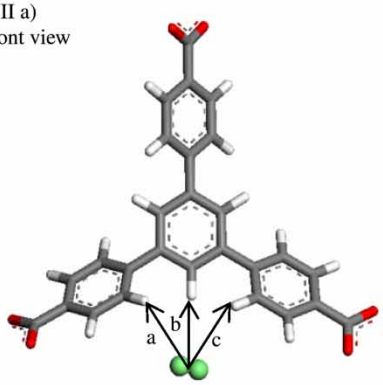

(VII b)
Side view

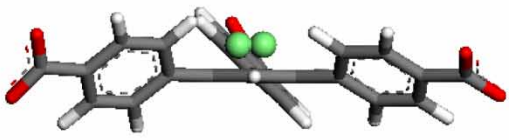

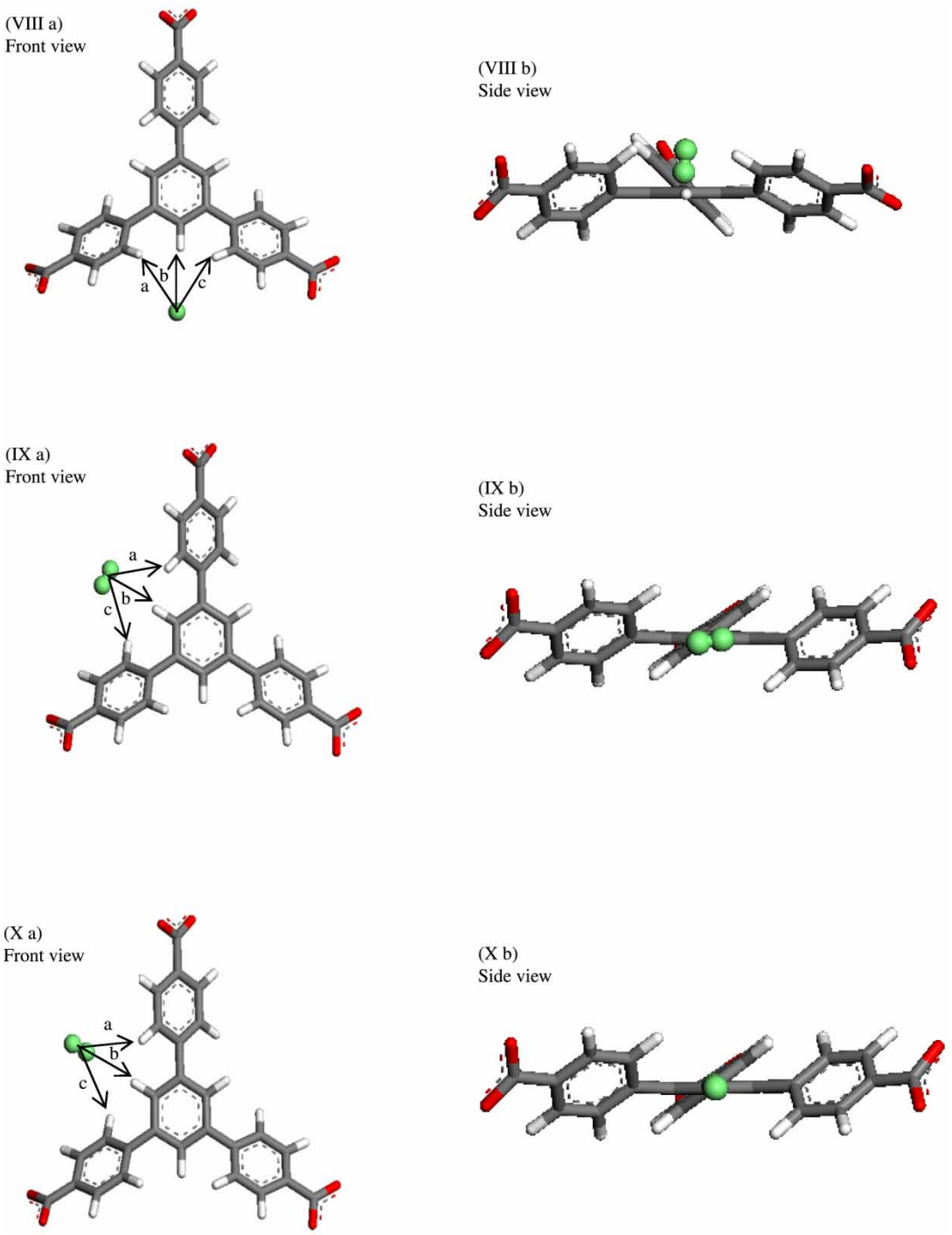

Figure 3. DFT-optimised structures of a H_2 molecule adsorbed on organic linkers. Model VII: $a = 3.150$ Å, $b = 3.023$ Å, $c = 3.019$ Å. Model VIII: $a = 3.104$ Å, $b = 3.169$ Å, $c = 3.020$ Å. Model IX: $a = 3.298$ Å, $b = 2.691$ Å, $c = 3.279$ Å. Model X: $a = 3.212$ Å, $b = 2.589$ Å, $c = 3.232$ Å. The atoms are coloured as follows: red, O; grey, C; white, H; green, H_2 molecule (colour online).

3.3 Comparison of H_2 binding energy with other systems

In our calculations, the strongest binding energies of 4.50 kJ mol^{-1} at the inorganic cluster and 3.8 kJ mol^{-1} at the organic linker were observed. Extrapolated *ab initio* (MP2) computations found the physisorption energy for hydrogen on graphene sheets to be 7.2 kJ mol^{-1}. But this value will be reduced by the entropy contribution (3.4 kJ mol^{-1}) and a penalty due to lower binding energies of different orientations and adsorption sites, to about

Table 1. Binding energies (BE) of single H_2 molecules interacting with the organic linker (BTB) in various binding sites and orientations.

Model	I	II	III	IV	V	VI	VII	VIII	IX	X
BE (kJ mol^{-1})	3.65	3.0	3.53	2.83	2.95	2.63	3.80	3.35	3.80	2.37
Distance (Å)	3.209	3.251	3.258	3.226	4.854	4.873	3.023	3.169	2.691	2.589

Note: The distances given are between the molecular centre of H_2 and the centre of the ring for models I–VI and the nearest hydrogen atom of the central ring for models VII–X.

2.5 kJ mol^{-1} at room temperature. However, the interlayer distance in graphite (3.354 Å) is too small for the intercalation of free hydrogen molecules with a dynamic diameter of 4.06 Å. Furthermore, the specific surface area of bulk graphite is too low, and therefore a practically hydrogen uptake cannot be observed [36]. The *ab initio* calculation on a carbon nanotube shows a H_2 adsorption energy of 12.8 kJ mol^{-1} at the outer surface, this effect is opposite for the inner walls, and strong physisorption of up to 30 kJ mol^{-1} has been claimed for adsorption sites close to the tip at the inside of nanotubes [37]. K-doped SWCNT shows the H_2 binding energy up to 14.2 kJ mol^{-1}, computed using the MP2 method [38], while Li-doped SWCNT shows the H_2 binding energy up to 19.7 kJ mol^{-1} calculated by the DFT method [35]. Theoretical studies have found that the interaction energy of H_2 molecules with the polarising centres of zeolites such as alkali-metal ions is in the range of 5.0–9.0 kJ mol^{-1} [39–41]. The highest experimental H_2 storage capacity reported is 1.8 wt% at 77 K and at 15 bar for zeolite NaY, whereas for sodalites, maximum capacities of less than 4.8 wt% H_2 are predicted based on thermodynamic optimisation

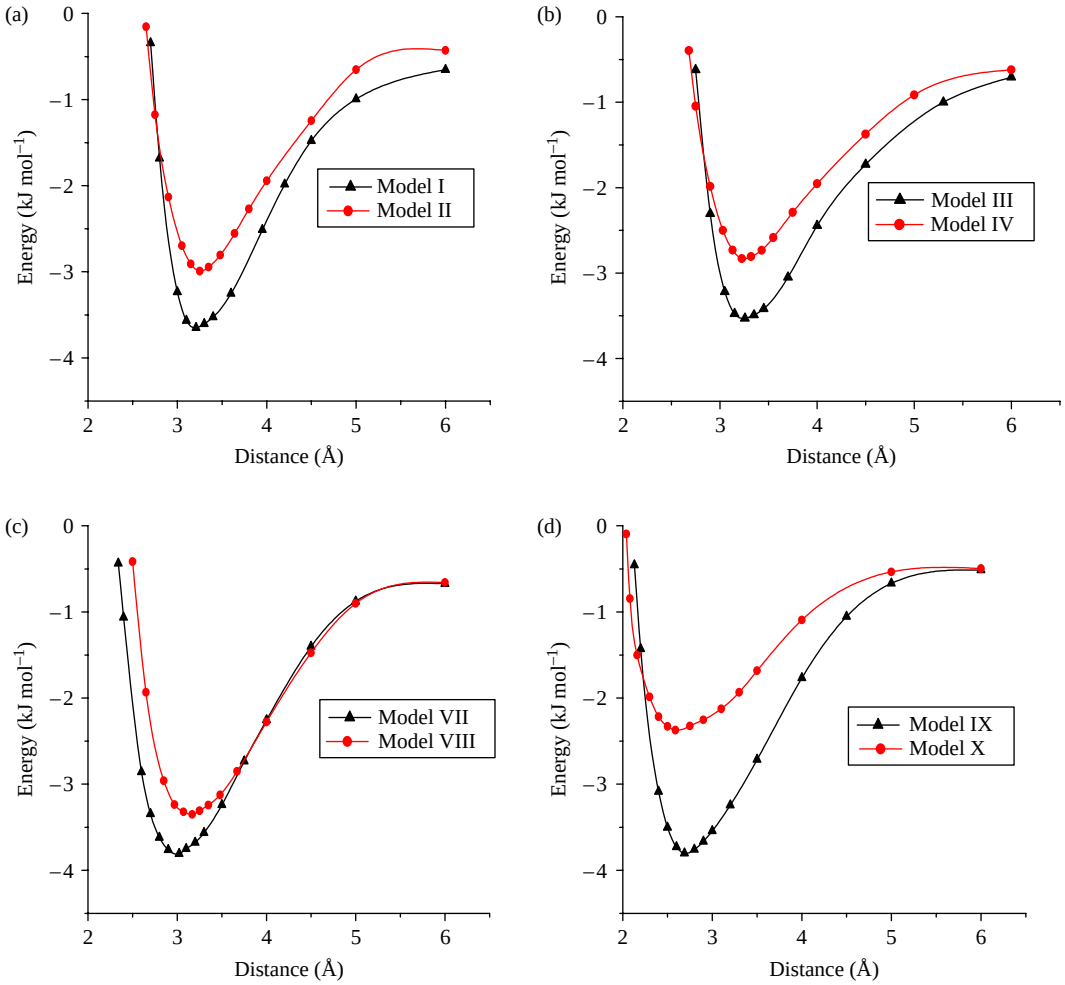

Figure 4. The interaction of H_2 with the MOF-177 organic linker as a function of the H_2–host distance for: (a) models I and II, (b) models III and IV, (c) models VII and VIII, (d) models IX and X. The corresponding model structures and adsorption sites are given in Figure 3.

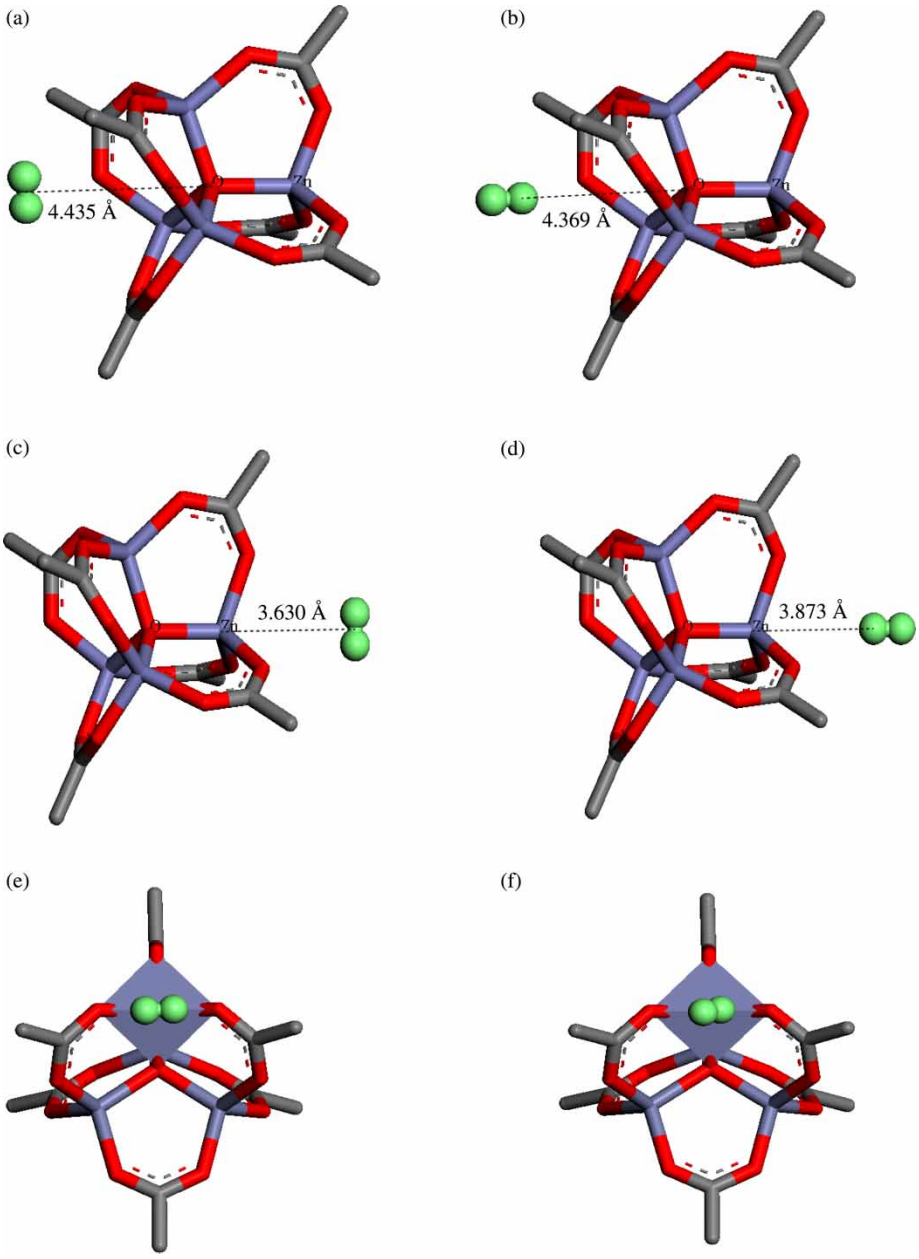

Figure 5. DFT-optimised structures of a H_2 molecule adsorbed over the α-, β- and γ-sites at the inorganic cluster. (a) H_2 in perpendicular orientation to the central O—Zn bond at the α-site. (b) H_2 in parallel orientation at the α-site. (c) H_2 in perpendicular orientation to the central Zn—O bond at the β-site. (d) H_2 in parallel orientation at the β-site. (e) H_2 in perpendicular orientation (with respect to the centre of the O—O edge of the ZnO_2 triangle) at the γ-site. (f) H_2 in parallel orientation at the γ-site. The atoms are coloured as follows: purple, Zn; red, O; grey, C; white, H; green, H_2 molecule (colour online).

and theoretical predictions [42,43], but even this is far from attainable at pressures below 30 bar. The H_2 interaction energy in zeolite is greater than that in the MOF but due to the small pore volume and surface area of zeolites than that of MOF, zeolite shows less H_2 storage capacity and is not suitable for practical interest as a storage material. The thermodynamic requirement for an adsorbent capable of storing hydrogen at ambient temperature should have the interaction energy of hydrogen equal to 15.1 kJ mol^{-1} [44].

3.4 Multiple H_2 binding

We also calculated the binding energies of multiple H_2 molecules interacting with the organic linker to investigate how the already adsorbed H_2 molecules effect the binding

Table 2. Binding energies (BE) of H_2 molecules interacting with the inorganic cluster in various binding sites and orientations.

Model	Adsorption site	BE (kJ mol^{-1})	Distance (Å)
a	α-Perpendicular	4.50	4.435
b	α-Parallel	2.96	4.369
c	β-Perpendicular	4.00	3.630
d	β-Parallel	4.24	3.873
e	γ-Perpendicular	3.95	4.283
f	γ-Parallel[a]	3.76	4.255

Note: The distances are given between the molecular centre of H_2 and central O atom for the α-site and nearest Zn atom for the β- and γ-sites. [a]There is a change in the relative orientation of the H_2 molecule during the geometry optimisation.

Table 3. Binding energies (BE) of multiple H_2 molecules interacting with the organic linker (BTB).

No. of H_2 molecules	Total BE (kJ mol^{-1})	CBE (kJ mol^{-1})
1	3.0	3.0
2	6.20	3.20
3	9.48	3.28
4	12.84	3.36
5	16.73	3.89
6	20.68	3.95
7	24.70	4.02

of further H_2 molecules. First, the geometry of the organic linker model was optimised, and then a single and up to seven H_2 molecules were placed at different positions on the organic linker and allowed to relax by geometry optimisation. The calculated total binding energies and consecutive binding energies are given in Table 3 and the multiple H_2 adsorbed on the organic linker is shown in Figure 6. Our result shows that, as the number of H_2 molecules increases, the CBE increases due to the interaction of H_2 molecules with the already adsorbed

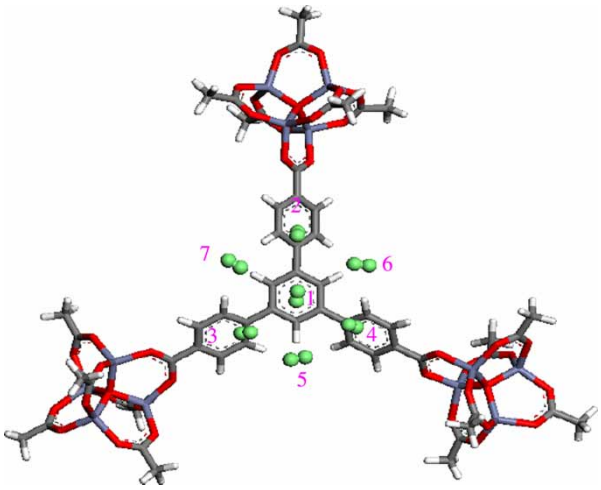

Figure 6. DFT-optimised structure of one to seven H_2 molecules adsorbed on the organic linker.

H_2 molecules. The CBE of the second H_2 is higher than the first H_2 and shows that the first adsorbed H_2 molecule favours the adsorption of the second H_2 molecule. The average distance between the adsorbed H_2 molecules is 3.3 Å. From the consecutive binding energies, we can conclude that the adsorption of multiple H_2 molecules is a favourable process if there are sufficient binding sites available, and the adsorbed molecules help in the binding of further H_2 molecules.

4. Conclusion

DFT calculations were carried out to find the binding energy of the H_2 molecule with the MOF-177 cluster. H_2 binding energy was evaluated at the inorganic cluster and the organic linker (BTB). The binding energy of H_2 observed at the inorganic cluster sites is in the order of $\alpha > \beta > \gamma$. The interaction of H_2 with the inorganic cluster was stronger than the organic linker (BTB); the estimated H_2 binding energy is 2.96–4.50 kJ mol^{-1} at the inorganic cluster and 2.6–3.8 kJ mol^{-1} at the organic linker. Both the organic linker and the inorganic cluster play an important role in the H_2 adsorption. Our results showed that the H_2 binding energy at the inorganic cluster was effected by the organic linker. The multiple H_2 molecules binding at the organic linker are also evaluated, and the results showed that the adsorbed molecule helps in the binding of further H_2 molecules. Due to the presence of more number of adsorption sites at the organic linker (BTB) and the strong interaction of H_2 with the inorganic cluster, MOF-177 showed higher H_2 adsorption capacity at 77 K. The calculated H_2 binding energies are far lower than the required values (15–50 kJ mol^{-1}), therefore the MOF-177 material is not suitable for room temperature H_2 storage. However, one can modify MOF by chemical treatment or functionalisation in such a way that hydrogen can be physically adsorbed with higher physisorption energies. Moreover, the MOF material with open metal sites in which H_2 molecules could approach the metal atoms more efficiently should also be a good hydrogen storage material.

Acknowledgement

The authors are thankful to the Council of Scientific and Industrial Research, New Delhi, for funding under network project.

References

[1] M.G. Nijkamp, J.E.M.J. Raaymakers, A.J. van Dillen, and K.P. de Jong, *Hydrogen storage using physisorption – materials demands*, Appl. Phys. A: Mater. Sci. Process. 72 (2001), pp. 619–623.
[2] M. Fichtner, *Nanotechnological aspects in materials for hydrogen storage*, Adv. Eng. Mater. 7 (2005), pp. 443–455.
[3] L. Schlapbach and A. Züttel, *Hydrogen-storage materials for mobile applications*, Nature 414 (2001), pp. 353–358.

[4] A. Züttel, *Materials for hydrogen storage*, Mater. Today 6 (2003), pp. 24–33.

[5] H. Li, M. Eddaoudi, M. O'Keeffe, and O.M. Yaghi, *Design and synthesis of an exceptionally stable and highly porous metal-organic framework*, Nature 402 (1999), pp. 276–279.

[6] D.J. Collins and H.C. Zhou, *Hydrogen storage in metal-organic frameworks*, J. Mater. Chem. 17 (2007), pp. 3154–3160.

[7] H.K. Chae, D.Y. Siberio-Pérez, J. Kim, Y.B. Go, M. Eddaoudi, A.J. Matzger, M. O'Keeffe, and O.M. Yaghi, *A route to high surface area, porosity and inclusion of large molecules in crystals*, Nature 427 (2004), pp. 523–527.

[8] A.G. Wong-Foy, A.J. Matzger, and O.M. Yaghi, *Exceptional H_2 saturation uptake in microporous metal-organic frameworks*, J. Am. Chem. Soc 128 (2006), pp. 3494–3495.

[9] J.L.C. Rowsell and O.M. Yaghi, *Strategies for hydrogen storage in metal-organic frameworks*, Angew. Chem., Int. Ed. 44 (2005), pp. 4670–4679.

[10] J.L.C Rowsell, E.C. Spencer, J. Eckert, J.A.K. Howard, and O.M. Yaghi, *Gas adsorption sites in a large-pore metal-organic framework*, Science 309 (2005), pp. 1350–1354.

[11] J.L.C. Rowsell, J. Eckert, and O.M. Yaghi, *Characterization of H_2 binding sites in prototypical metal-organic frameworks by inelastic neutron scattering*, J. Am. Chem. Soc. 127 (2005), pp. 14904–14910.

[12] T. Yildirim and M.R. Hartman, *Direct observation of hydrogen adsorption sites and nanocage formation in metal-organic frameworks*, Phys. Rev. Lett. 95 (2005), p. 215504.

[13] E.C. Spencer, J.A.K. Howard, G.J. McIntyre, J.L.C. Rowsell, and O.M. Yaghi, *Determination of the hydrogen absorption sites in Zn_4O (1,4-benzenedicarboxylate) by single crystal neutron diffraction*, Chem. Commun. (2006), pp. 278–280.

[14] T. Sagara, J. Klassen, and E. Ganz, *Computational study of hydrogen binding by metal-organic framework-5*, J. Chem. Phys. 121 (2004), pp. 12543–12547.

[15] G. Garberoglio, A.I. Skoulidas, and J.K. Johnson, *Adsorption of gases in metal-organic materials: Comparison of simulations and experiments*, J. Phys. Chem. B 109 (2005), pp. 13094–13103.

[16] A.I. Skoulidas and D.S. Sholl, *Self-diffusion and transport diffusion of light gases in metal-organic framework materials assessed using molecular dynamics simulations*, J. Phys. Chem. B 109 (2005), pp. 15760–15768.

[17] Q. Yang and C. Zhong, *Molecular simulation of adsorption and diffusion of hydrogen in metal-organic frameworks*, J. Phys. Chem. B 109 (2005), pp. 11862–11864.

[18] Q. Yang and C. Zhong, *Understanding hydrogen adsorption in metal organic frameworks with open metal sites: A computational study*, J. Phys. Chem. B 110 (2006), pp. 655–658.

[19] H. Frost, T. Du1ren, and R.Q. Snurr, *Effects of surface area, free volume, and heat of adsorption on hydrogen uptake in metal organic frameworks*, J. Phys. Chem. B 110 (2006), pp. 9565–9570.

[20] T. Sagara, J. Klassen, J. Ortony, and E. Ganz, *Binding energies of hydrogen molecules to isoreticular metal-organic framework materials*, J. Chem. Phys. 123 (2005), pp. 14701–14704.

[21] C. Buda and B.D. Dunietz, *Hydrogen physisorption on the organic linker in metal organic frameworks:* Ab initio *computational study*, J. Phys. Chem. B 110 (2006), pp. 10479–10484.

[22] T.B. Lee, D. Kim, D.H. Jung, S.B. Choi, J.H. Yoon, J. Kim, K. Choi, and S.H. Choi, *Understanding the mechanism of hydrogen adsorption into metal organic frameworks*, Catalysis Today 120 (2007), pp. 330–335.

[23] E. Klontzas, A. Mavrandonakis, G.E. Froudakis, Y. Carissan, and W. Klopper, *Molecular hydrogen interaction with IRMOF-1: A multiscale theoretical study*, J. Phys. Chem. C 111 (2007), pp. 13635–13640.

[24] D. Kim, D.H. Jung, S.B. Choi, J.H. Yoon, J. Kim, K. Choi, and S.H. Choi, *A density functional theory study on the interaction of hydrogen molecules with aromatic linkers in metal organic frameworks*, J. Phys. Chem. Solids 69 (2008), pp. 1428–1431.

[25] A. Kuc, T. Heine, G. Seifert, and H.A. Duarte, *On the nature of the interaction between H_2 and metal organic frameworks*, Theor. Chem. Account 120 (2008), pp. 543–550.

[26] *Materials Studio*, *Version 4.2*, Accelrys Software, Inc., San Diego, 2007.

[27] J.P. Perdew and Y. Wang, *Accurate and simple analytic representation of the electron-gas correlation energy*, Phys. Rev. B 45 (1992), pp. 13244–13249.

[28] B. Delley, *An all-electron numerical method for solving the local density functional for polyatomic molecules*, J. Chem. Phys. 92 (1990), pp. 508–517.

[29] B. Delley, *Fast calculation of electrostatics in crystals and large molecules*, J. Phys. Chem. 100 (1996), pp. 6107–6110.

[30] B. Delley, *From molecules to solids with the DMol(3) approach*, J. Chem. Phys. 113 (2000), pp. 7756–7764.

[31] N.A. Ramsahye, G. Maurin, S. Bourrelly, P.L. Llewellyn, C. Serre, T. Loiseau, T. Devic, and G. Férey, *Probing the adsorption sites for CO_2 in metal organic frameworks materials MIL-53 (Al, Cr) and MIL-47 (V) by density functional theory*, J. Phys. Chem. C 112 (2008), pp. 514–520.

[32] S. Bhattacharya, C. Majumder, and G.P. Das, *Hydrogen storage in Ti-decorated BC4N nanotube*, J. Phys. Chem. C 112 (2008), pp. 17487–17491.

[33] F. Tran, J. Weber, T.A. Wesołowski, F. Cheikh, Y. Ellinger, and F. Pauzat, *Physisorption of molecular hydrogen on polycyclic aromatic hydrocarbons: A theoretical study*, J. Phys. Chem. B 106 (2002), pp. 8689–8696.

[34] F. Negri and N. Saendig, *Tuning the physisorption of molecular hydrogen: Binding to aromatic, hetero-aromatic and metal-organic framework materials*, Theor. Chem. Account 118 (2007), pp. 149–163.

[35] J.H. Cho and C.R. Park, *Hydrogen storage on Li-doped single-walled carbon nanotubes: Computer simulation using the density functional theory*, Catalysis Today 120 (2007), pp. 407–412.

[36] T. Heine, L. Zhechkov, and G. Seifert, *Hydrogen storage by physisorption on nanostructured graphite platelets*, Phys. Chem. Chem. Phys. 6 (2004), pp. 980–984.

[37] Y. Okamoto and Y. Miyamoto, Ab initio *investigation of physisorption of molecular hydrogen on planar and curved graphenes*, J. Phys. Chem. B 105 (2001), pp. 3470–3474.

[38] G.E. Froudakis, *Why alkali-metal-doped carbon nanotubes possess high hydrogen uptake*, Nano Lett. 1 (2001), pp. 531–533.

[39] F.J. Torres, J.G. Vitillo, B. Civalleri, G. Ricchiardi, and A. Zecchina, *Interaction of H_2 with alkali-metal-exchanged zeolites: A quantum mechanical study*, J. Phys. Chem. C 111 (2007), pp. 2505–2513.

[40] C.O. Arean, G.T. Palomino, E. Garrone, D. Nachtigallova, and P. Natchtigall, *Combined theoretical and FTIR spectroscopic studies on hydrogen adsorption on the zeolites Na-FER and K-FER*, J. Phys. Chem. B 110 (2006), pp. 395–402.

[41] P. Natchtigall, E. Garrone, G.T. Palomino, G. Rodrıguez, M. Delgado, D. Nachtigallova, and C.O. Arean, *FTIR spectroscopic and computational studies on hydrogen adsorption on the zeolite Li–FER*, Phys. Chem. Chem. Phys. 8 (2006), pp. 2286–2292.

[42] J.G. Vitillo, G. Ricchiardi, G. Spoto, and A. Zecchina, *Theoretical maximal storage of hydrogen in zeolitic frameworks*, Phys. Chem. Chem. Phys. 7 (2005), pp. 3948–3954.

[43] W.C. van den Berg, S.T. Bromley, and J.C. Jansen, *Thermodynamic limits on hydrogen storage in sodalite framework materials: A molecular mechanics investigation*, Microporous Mesoporous Mater. 78 (2005), pp. 63–71.

[44] S.K. Bhatia and A.L. Myers, *Optimum conditions for adsorptive storage*, Langmuir 22 (2006), pp. 1688–1700.